

## **ASSESSMENT OF THE SEISMIC BEHAVIOR OF THE STEEL COUPLING BEAMS IN COUPLED SHEAR WALLS IN STEEL STRUCTURES AT TARGET DISPLACEMENT POINT**

**Farrokh Forootan, Dr Moghadam**

Science and Research Branch, Islamic Azad University, Tehran, Iran.

### **ABSTRACT**

Concrete Coupling beam in coupled shear walls is a first line of defense, and acts as a fuse shear operation, and the first plastic hinge formed in it. So its appropriate behavior to improve the performance of the structure against earthquakes is of great importance. Due to the complex and time-taking nature of the construction and operation of diagonal reinforcement in concrete coupling beams, steel coupling beams are the alternative to the beam. Accordingly, in this paper, the structures of 12 and 22 floors were designed with twin side load bearing system coupled shear wall with steel coupling beam and Flexural steel frame, and the seismic behavior of coupled shear walls and steel coupling beams in the two structures were evaluated. The results show that the direction of the moment of shear walls at the height of the structure has changed (joint formation in height), which results in the waste of a lot of energy. The seismic behavior of the coupled steel beams in the shear walls of the steel structures at the target displacement point in the linear analysis and the seismic DBE is assessed, while the proportion of the steel moment frame and the yield shear walls is about 15% and 85%, respectively, however, this amount reaches more than 30% at the target displacement point in the nonlinear static analysis. In addition, according to the results of seismic DBE, the coupled beams in a 22-storey structure is more consistent with the results of the nonlinear static analysis compared with the 12-storey structure.

**KEYWORDS:** target displacement; coupled shear walls; steel coupling beams; nonlinear static analysis.

### **1. Introduction**

Coupled shear wall systems is considered as a lateral load system and has a very good performance against lateral loads caused by earthquake and wind. To create a system of coupled shear walls, we can connect separate shear walls by means of coupled beams in the open area coupled between the walls and the floor level of the structure. The coupled shear wall system can, in case of a regular pattern of openings located at an altitude between shear walls and properly designed coupled beams, provide sufficient hardness resistance against lateral loads. In separate shear walls, the Overturning Moment of the structure is carried out by flexural structures created in the walls and the absorbing of the earthquake input energy by flexural the joint creation of the walls (walls with a high ratio of height to length) or joint shear walls in between floors (walls with a low ratio of height to length). When the coupled shear wall system lies in the lateral load, shear forces at the ends of coupled beams emerge in opposite directions. By closing the shear walls with coupled beams, a large percentage of the total overturning moment of the structure will be applied to the pair of axial forces caused by tensional-compressive forces (caused by coupled arrows) of the walls, which is a more appropriate mechanism compared to that of separate shear walls.

If the coupled beams are correctly in proportion to the total height of the coupled shear wall system, the beams absorb the seismic energy input by forming shear joints (Aktan and Bertero 1981, Aristizabal-Ochoa 1982). If the coupled beam energy is absorbed correctly along the height of the structure, the seismic energy dissipation structures will be at full height. This is very desirable compared to the separate walls in which the wasted energy is concentrated at the foot of the wall (Park and Paulay 1975, Fintel and Ghosh 1982, Aktan and Bertero 1984). In the past, several types of coupled beams have been studied by researchers. Among the tested coupled beams, Steel-Concrete Composite Coupling Beams and Diagonally Braced Reinforced Concrete Coupling Beams have been investigated more than other types of beams. Concrete coupling beams with diagonal reinforcement require rather difficult and precise details for good performance. Special conditions for determining the details of the concrete coupling beam in connection to the shear wall and the need to connect to a compact transverse reinforcement along the length of the diagonal reinforcement introduce challenges in the implementation of this type of coupling beams. Thus, to steel coupling beams were introduced as an alternative for coupling concrete beams. The design of Steel coupling beams at the coupled shear wall bracing coupling beams is carried out in the Eccentrically-Braced Frame. Investigation by Harries and his colleagues in the mid-90s (Harries et al. 1993, Harries et al. 1995) showed that the bracing coupling beams topologies which are designed based on eccentrically-braced Frame beams indicate desirable formation energy absorption characteristics against the reciprocating loads. Research conducted by park and Yun (Park and Yun 2005a, Park and

Yun 2005b, Park and Yun 2006a) on 3 samples showed that if the coupling steel beam is designed based on the shear submission, it will have the ability to absorb much more energy and more stable hysteresis behavior compared to steel coupling beams designed based on the submission of coupled strength. The investigation also found that in the presence of auxiliary transmission reinforcement and Horizontal Ties area where the coupling beam is placed in the wall, the point where the steel coupling beam is fixed inside the wall, is located inside the wall at an approximate distance of one-fifth or one-sixth the length of the beam position on the outer side of the shear wall. El-Tawil et al (El-Tawil et al. 2002, El-Tawil and Kuenzli 2002) studied parameters in the structural behavior of coupled shear walls. In this study, the structural behavior was studied by the nonlinear static analysis on the structure of the coupling ratio wall. In this study, El-Tawil et al designed four 12 floor structures, and four 6 floor structures with coupling ratios of 0, 30, 45 and 60%. In these Structures, only the system of coupled shear walls and coupling beams was considered and the steel frame was ignored. Modeling of structures was carried out using the Finite- Element Model. The effects of different topology ratios were presented on the structural behavior. In a study, Fortney (Fortney 2005) compared the behavior of coupled shear wall structural with steel coupling beams and coupled shear walls with concrete coupling beams. Both structures had 20 floors and the time history analysis was used to examine their behavior. In this study, for the nonlinear dynamic analysis, the steel Flexural frames were ignored and only the shear wall was considered as the side load bearing element.

**2. Modeling and Design**

**2.1 linear Modeling and Design of 12 and 22 Floor Structures**

In most research done on the seismic behavior of coupled shear wall with coupling steel beams of the steel frame is ignored. In this paper, two groups of 12 and 22-floor structures are used with dual coupled shear wall system with coupling steel beams and steel moment frame, has three spans 7.7 m in the direction of X and Y. 3.24 m is the height of each floor. The structural plans are shown In Fig. 1. All the design parameters including behavior coefficient (R) and the coefficient of resistance ( $\Omega_0$ ) have been considered 7 and 2.5, respectively, in accordance with ASCE 7-05 and FEMA-450. Floor and roof dead loads were considered 7500 N/m<sup>2</sup>, the floors’ live load was considered 2000 N/m<sup>2</sup>, and the roof live load was considered 1500 N/m<sup>2</sup>. Compressive strength of concrete shear walls was considered 40MPa, the yield strength of steel was considered 235Mpa, the flexural and shear reinforcement yield were considered 400MPa and 300MPa, respectively.

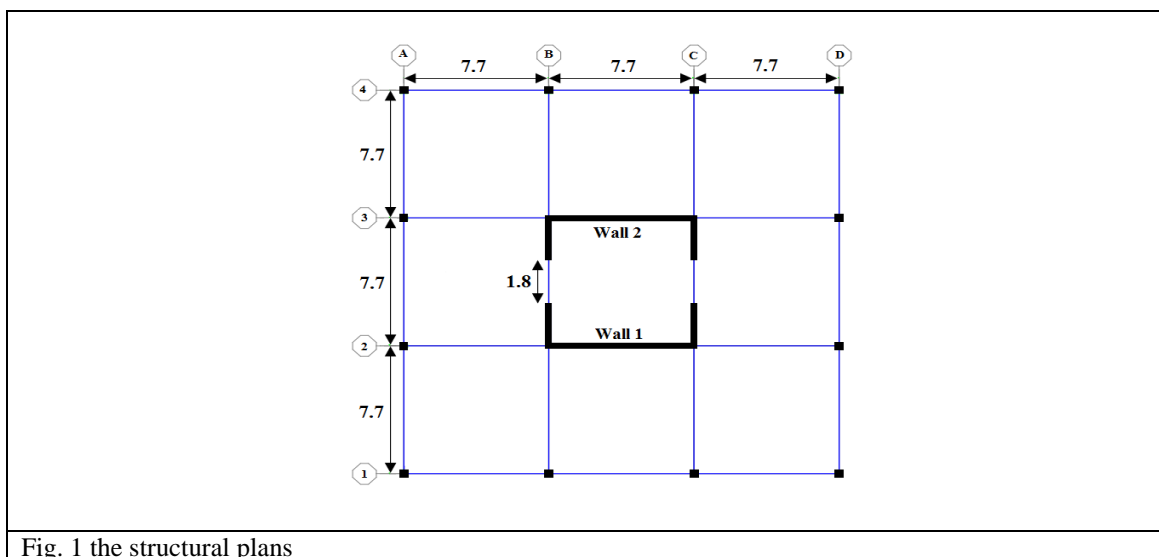


Fig. 1 the structural plans

In order to Model and linearly analyze the two 12 and 22 floor structures, the ETABS (Computers and Structures Inc. Version 9.7.3) software was used. To consider the effects of shear cracks in the wall, according to ACI 318-05, the flexural stiffness of shear walls of the first and second floors were multiplied by the reduction factor 0.35. The connection of beams and steel frame beams was assumed neutral. At the junction of the wall shear beams of steel moment frames, due to the lack of adequate enforcement to obtain fixed, it was assumed that the joint is the junction

beam steel frame to the wall. The connection of steel coupling beam to the concrete shear wall was assumed to be tangly. In these designs, it is assumed that the tangly point of the steel coupling beam is located on the outer side of the wall. Designing the steel Flexural frame beams was carried out according AISC99- LRFD. In accordance with the Regulations concerning framed structures with dual bearing walls, steel moment frame have to be able to resist 25% of the earthquake loads of the project without the shear walls. In designing the steel moment frame columns, the columns were designed in the shape of a cross. In Fig. 2, the Schematic view of columns designed for the structures is presented. Table 1-2 provide the types of steel moment frame beams and columns of the 12 and 22 floor structures, respectively. Also, Dimensions and types of steel coupled beams in terms of height are presented in the table 3.

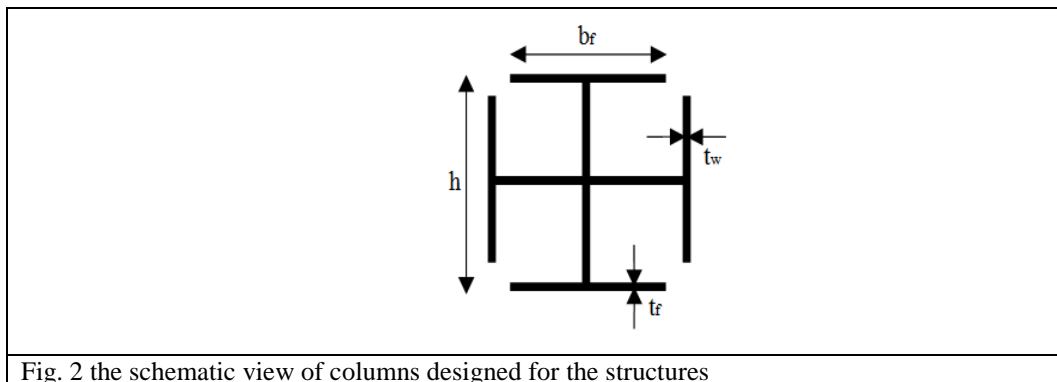


Fig. 2 the schematic view of columns designed for the structures

Table 1 the types of steel moment frame beams of the 12 and 22 floor structures

22 floor structure		12 floor structure					
In the direction of X		In the direction of Y		In the direction of X		In the direction of Y	
Corner Beams	Intermediate Beams						
IPB 360	IPB 260	IPB 450	IPE 240	IPB 280	IPB 300	IPB 360	IPE 300

Table 2 the types of steel moment frame columns of the 12 and 22 floor structures

Column Name	h	d	bf	tf	tw
SALIBI 1	80	74	55	3	3
SALIBI 2	70	64	40	3	12
SALIBI 3	60	54	36	3	1.2

Table 3 Dimensions and types of steel coupling beams of the 12 and 22 floor structures

Section Name	22 floor structure			12 floor structure	
	Floor 2-7	Floor 8-16	Floor 17-22 & 1	Floor 2-7	Floor 8-12 & 1
CB 1-22	CB 2-22	CB 3-22	CB 1-12	CB 2-12	
h	70	55	40	51	35
bf	20	18	16	18	16
tf	3.6	4	2.8	4	2.8
tw	1	0.8	0.5	0.8	0.8
V <sub>p, Flexure (KN)</sub>	1507	1075	474	981	442
V <sub>p, Shear (KN)</sub>	886	530	242	485	332
V <sub>n (KN)</sub>	886	530	242	485	332

Flexural design of shear wall was done in accordance with the regulations of ACI 318-05. The ratio of demand to flexural capacity for shear walls of the two structure was placed in the range of 0.6 to 0.8 after being designed (except

in upper floors where the ratio is about 0.3 to 0.4). Shear design of shear walls was done manually according to the regulations of ACI 318-05. Due to intermittent exposure of coupled shear walls to tension and compression, the shear strength of the concrete wall was ignored, and the strength of transverse reinforcement was considered in the design of shear walls. The thickness of the shear walls for the 12 and 22 floor structures is presented in Table 4.

**Table 4 the thickness of the shear wall for the 12 and 22 floor structures**

	22 floor structure				12 floor structure	
	Floor 1-4	Floor 5-7	Floor 8-14	Floor 15-22	Floor 1-4	Floor 5-12
$t_{wall}$	70	60	45	30	30	25

## 2.2 Non- linear Modeling and Design of 12 and 22 Floor Structures

In the non-linear model, the resistance of the material is considered as the expected resistance. To determine the expected resistance of concrete and steel, nominal values for the yield strength of steel and maximum concrete compressive stress are multiplied in 1.25 and 1.5, respectively. In order to model the shear walls in the software, concrete walls and steel reinforcement materials have been selected as Concrete01 and Steel02, respectively. Concrete01 is available in based on the concrete model Kent-Scott-Park in the OpenSees software. In this model, the tensile strength of concrete is equal to zero. Compressive strength of confined and non-confined concrete are considered  $6.6 \times 10^7 \text{ N/m}^2$  and  $5.0 \times 10^7 \text{ N/m}^2$ , respectively, and ultimate compressive strength of the concrete is considered to be 2.0 of the maximum compressive strength of confined and non-confined concrete. The confined concrete strain at the maximum compressive strength and ultimate compressive strength should be considered 0.5% and 2.5%, respectively. Also Steel02 is available in the OpenSees software based on the steel model Giuffre-Menegotto-Pinto. Since the main focus of the research is the nonlinear behavior of coupled shear walls coupled with steel beams, nonlinear analysis was performed in order to reposition it on the side bearing structures (in the direction of Y). In the research, for modeling and analysis of nonlinear structures the OpenSees software was used. Because of the symmetry of the structure plan, in order to reduce the operation time, only half of the structure was modeled in two dimensions in Open Sees. In the modeling of linear structures, the connection of beam steel frame to the shear wall was considered in detail. Given this assumption, in the modeling of nonlinear structures, frame A12, A23 and A34 are considered as moment frames and the frames B12 and B34 as simple frame responsible for Burberry's gravity.

To model the coupled shear wall in the software OpenSees, the equivalent frame method is used. In this method the shear column is modeled in the form of a column and the specifications of the shear section will be dedicated to the column. In the equivalent frame method, the equivalent column to which the shear wall section specifications are dedicated is placed in the area center of the shear wall. To consider the actual length of the shear walls and constant coupled beam length, the ends of the beam have to be attached to the sides of the beam by the beam spinal columns. the connection of the steel coupling beams to these beams is tangly rigid. In Fig. 3 the modeling of coupled shear walls and steel coupling beams is displayed.

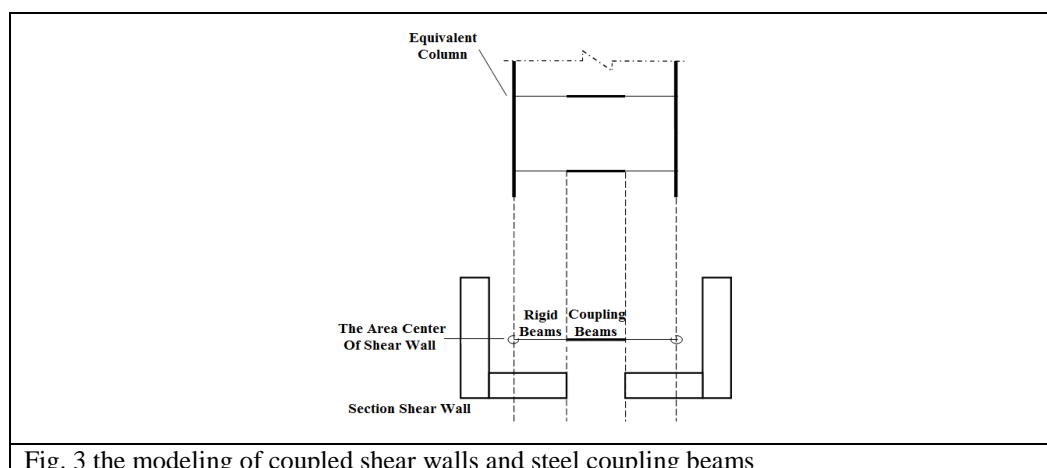


Fig. 3 the modeling of coupled shear walls and steel coupling beams

Each of the structures at the tow level of the design earthquake (DBE) and the maximum expected earthquake (MCE), and at each level of earthquake, will be analyzed using 10 far-field accelerograms; hence 10 far-field accelerograms were selected based on the regulations of FEMA 450. Table 5 provides the Selectivity accelerograms for time history analysis.

Table 5 the Selectivity accelerograms for time history analysis

Earthquake Name	Magnitude	$g(m/s^2)$	Year of occurrence	Station
Northridge	6.7	0.48	1994	Canyon Country
Imperial Valley	6.5	0.38	1979	El Centro
Kobe, Japan	6.9	0.5	1995	Nishi- Akashi
Manjil, Iran	7.4	0.5	1990	Abbar
Chi-Chi, Taiwan	7.6	0.44	1999	CHY101
Duzce, Turkey	7.1	0.73	1999	Bolu
Friuli, Italy	6.5	0.31	1976	Tolmezzo
Landers	7.3	0.42	1992	Coolwater
Loma Prieta	6.9	0.44	1989	Capitola
Hector Mine	7.1	0.34	1999	Hector

To use accelerograms the acceleration values have to be scaled based on the design variety. In order to scale the accelerograms, the Regulations of ASCE 7-05 were used. According to the bylaws, first the standard design range (DBE) and the maximum range of the expected earthquake (MCE) are determined. In the next step, by applying values to the acceleration values of each of the accelerograms, the acceleration response spectrum for each mapping will be determined by considering the attenuation of 5%. Selectivity coefficients for the scale of earthquake accelerograms are presented for both DBE and MCE in Table 6.

Table 6 Selectivity coefficients for the scale of earthquake accelerograms

	Hecto r	Loma. .	Lande .	Friuli	Duzce	Chi.	Manji l	Kobe	Imper .	North.
DBE	2	2	1.74	2.1	0.96	1.8	0.91	1.77	1.84	1.476
MCE	2	2.2	2.2	2.1	1.8	1.8	2.2	1.77	2.2	2.2

### 3. The results of the static linear analysis

#### 3.1 Axial Force on Shear Wall

The maximum compressive force on each floor occurs when all coupling steel beams on the higher floors give up and the direction of the shear force applied by the beam on the wall is aligned with the weight force of the wall. The highest tensile force per floor occurs when the all-steel coupling beams in the higher floors give up and the beam shear force applied by the beam on the wall is in the opposite direction to the weight of the wall. As it can be seen in the linear analysis of 12 and 22 floor structures, shear walls do not stretch in any of the floors to stretch. Fig. 4 and 5 show the axial force of the shear walls on each floor of the 12 and 22 floor structures, respectively.

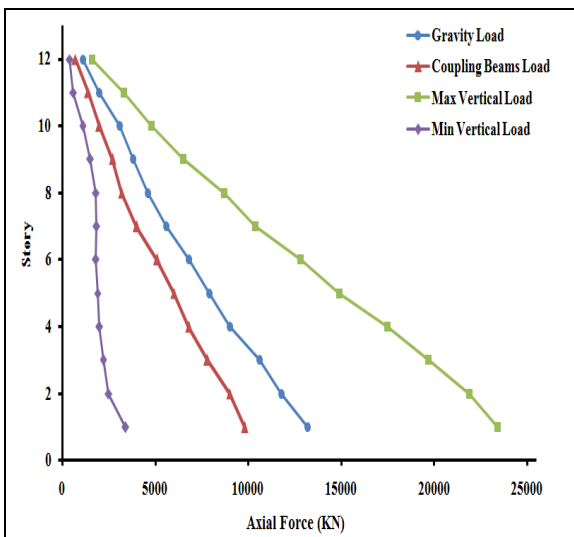


Fig. 4 axial force of the shear walls on each floor of the 12 floor structure

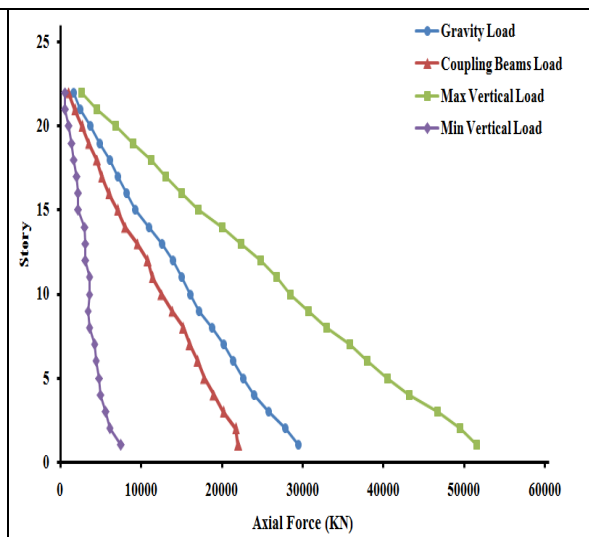


Fig. 5 axial force of the shear walls on each floor of the 22 floor structure

### 3.2 Moment in Shear Wall

On the fourth floor of the 12-floor structure and on the tenth floor of the 22-floor structure, the direction of the moment against the shear walls changes, and thus there is a possibility of the formation of the joint at the height of the wall. Fig. 6 and 7 display the flexural moment of the shear walls on each floor of the 12 and 22 floor structures under the load of EY, respectively.

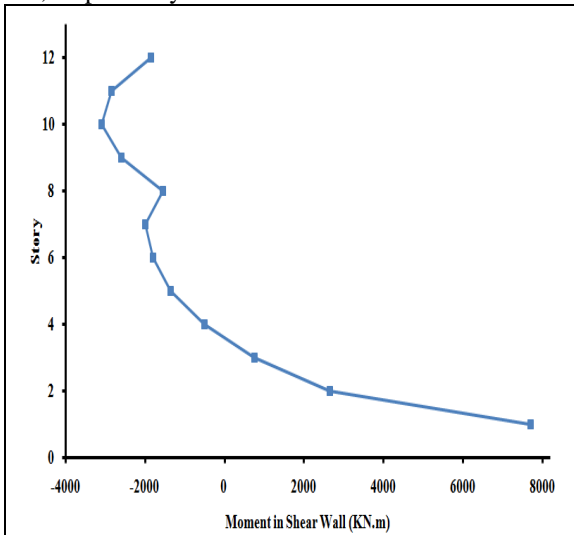


Fig. 6 flexural moment of the shear walls on each floor of the 12 floor structure

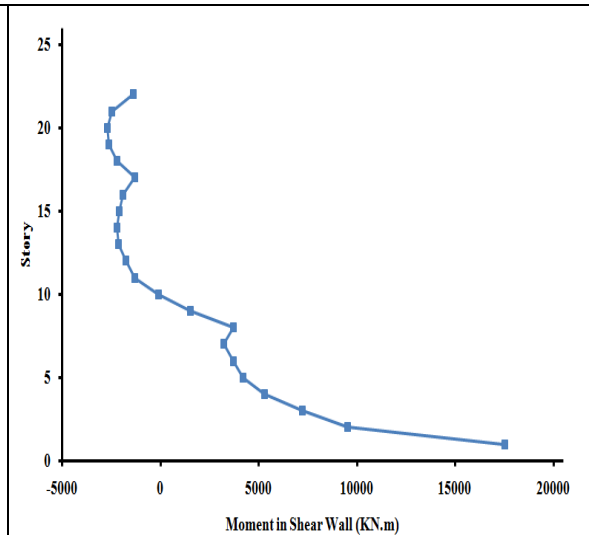


Fig. 7 flexural moment of the shear walls on each floor of the 22 floor structure

### 3.3 Maximum Shear in Coupling Beams

Fig. 8 and 9 show the maximum shear applied to the coupling steel beams in the 12 and 22 floor structures, respectively. To ensure the surrender of coupling steel beams and also to reduce the axial force generated by the coupling beam to the shear walls, the demand to capacity ratio is greater than 1 in most beams designed coupled 12 and 22 floor structures (El-Tawil et al. 2010).

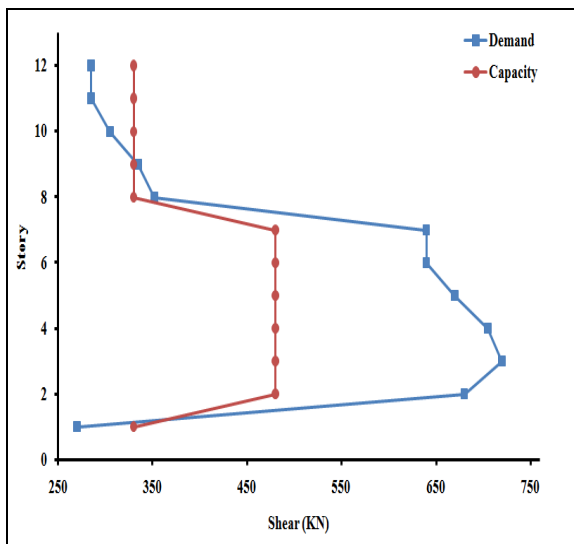


Fig. 8 maximum shear applied to the coupling steel beams in the 12 floor structure

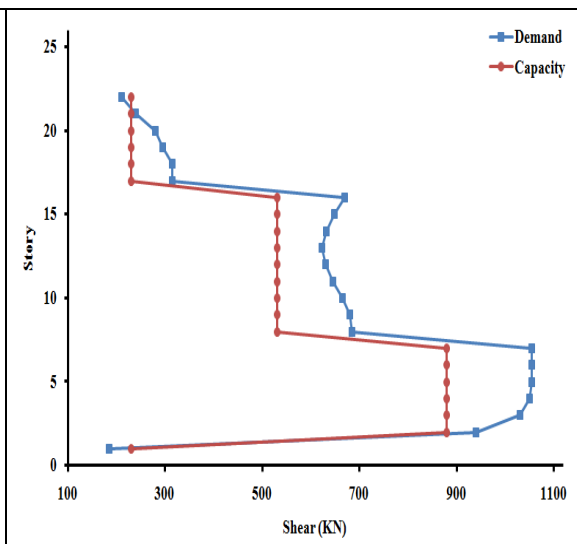


Fig. 9 maximum shear applied to the coupling steel beams in the 22 floor structure

#### 4. Nonlinear static analysis results

In the calculation of the ultimate displacement of the target structure, it is necessary to calculate the effective rigidity of the structure as the basis of the calculations, whereas the effective rigidity of the structure is a function of the target displacement. Therefore, in general, it is necessary to begin at the initial displacement status of the structure and calculate by using a repetition approach and modify the effective rigidity at each phase. In the nonlinear static analysis of the both 12- and 22-storey structures, the lateral load distribution model of the structure is based on the first status of the both structures and the both structures have had the relative lateral ceiling displacements at 3.5% and 3%, respectively. The target displacement is obtained in accordance with the regulations of FEMA-450 in Eqn (1).

$$\delta_r = C_0 \cdot C_1 \cdot C_2 \cdot C_3 \cdot S_a \cdot \frac{T_s^2}{4\pi^2} \cdot g \quad (1)$$

#### Assessment of basic shear diagram – ceiling displacement

As previously noted, the half of the original structure is considered in the non-linear model, therefore, for the calculation of the same displacement of the ceiling, the basic shear yield obtained from non-linear model should be compared with the half of the basic linear analysis. In Figures 10 and 11, the basic ceiling shear-displacement diagram of the both 12- and 22-storey structures is shown.

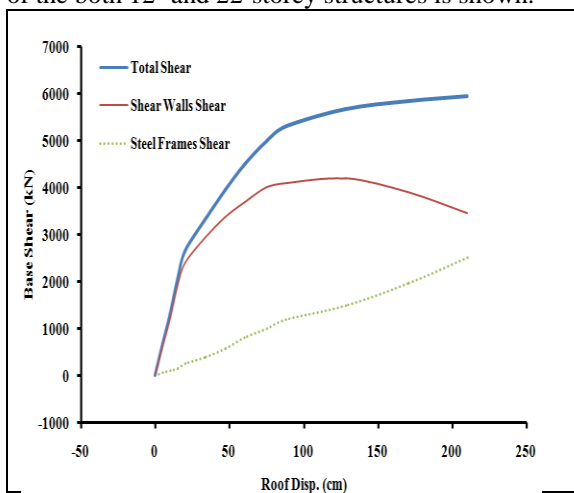


Fig. 10 the basic ceiling shear-displacement diagram of the 12 storey structures

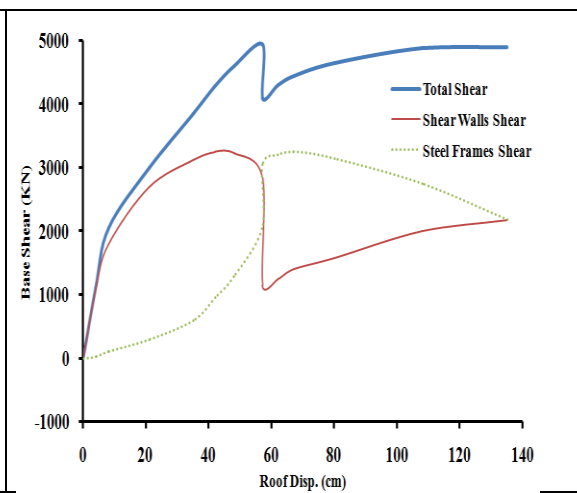


Fig. 11 the basic ceiling shear-displacement diagram of the 22 storey structures

As it can be seen, the shear behavior diagram of the basic-displacement status in the both 12- and 22-storey structures are the same. In the low relative displacements, the shear wall percentage in the basic shear section is much more compared with the steel flexural frames. However, the percentage of the steel ceiling flexural frames increases, when relative the displacement increases. In the case of the relative displacement, which is assumed as the relative allowed displacement in the linear analysis, while the percentage of the steel flexure frames and the coupled shear walls based on the non-linear static analysis of the 12-storey is 41% and 59%, respectively, and 33% and 67% for 22-storey on the total base shear. As it can be seen in the diagram, when the relative lateral ceiling increases, the percentage of the steel flexure frames of the total shear increases.

**Behavior assessment of steel coupling beams**

In Figures 12 and 13, the maximum rotation of the steel coupled beams are shown in the different storey in the 12- and 22-storey structures on the various relative displacements.

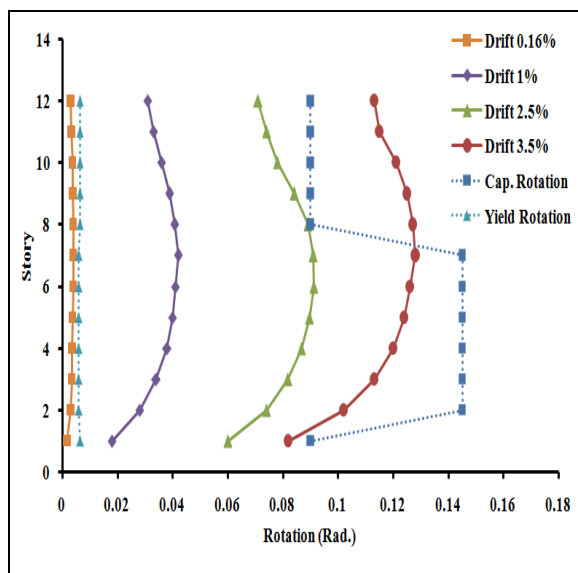


Fig. 12 the basic ceiling shear-displacement diagram of the 12 storey structures

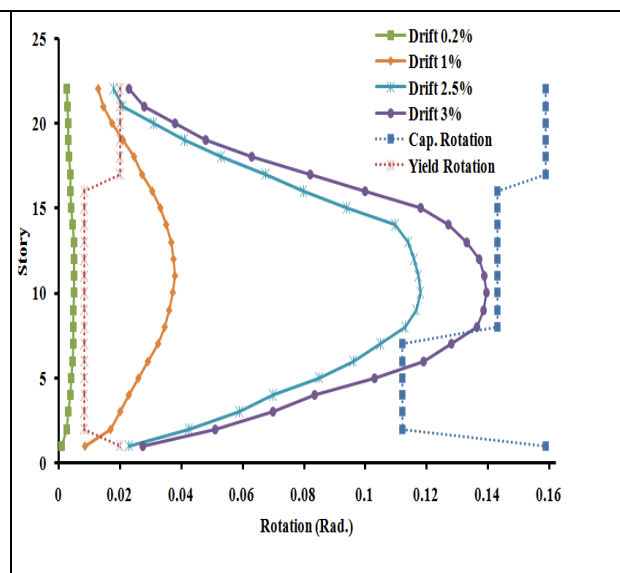


Fig. 13 the basic ceiling shear-displacement diagram of the 22 storey structures

In the case of 22-storey structure, as it can be seen, the relative displacement change is 0.2% (in respect to the roof displacement in the linear analysis), none of the coupled beams has reached yield point. In relative one percent (1%) displacement, except the first storey and several upper storey is over than other storey. In relative 2.5% displacement, the allowed displacement in the linear analysis almost includes all of the coupled beams that have reached the yield point and similar to the previous status of the shear coupled beam in the middle floors, which is more than the other floors and the relative 3.0% beams in the middle floors, has almost reached the rotation its maximum strength and, similar to the previous status patterns, the rotation in the middle classes is more than the other floors.

**4. The results of the Dynamic non- linear analysis**

**4.1 Axial Force on Shear Wall**

Shear walls no. 1 and 2 will not stretch in the 12-floor structure under the earthquake of DBE and MCE, but in the 22-floor structure, they have experienced slightly higher tensile axial force from the 10<sup>th</sup> floor up. Fig. 14 and 15 show the mean maximum and minimum axial forces exerted on the shear wall no. 1 under the earthquake of DBE and MCE for the 12 and 22-floor structures, respectively.

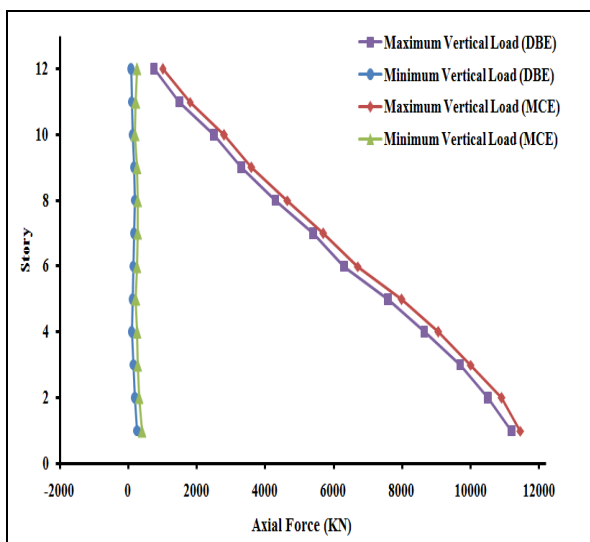


Fig. 14 mean maximum and minimum axial forces exerted on the shear wall no. 1 under the earthquake of DBE and MCE for the 12 floor structure

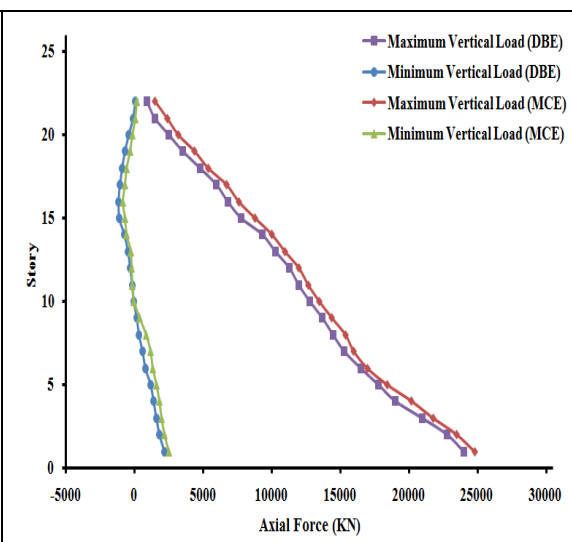


Fig. 15 mean maximum and minimum axial forces exerted on the shear wall no. 1 under the earthquake of DBE and MCE for the 22 floor structure

4.2 Moment of Shear Wall

For the 12-floor structure, the changes of the moment around strong and weak flexural moment are intense in the walls of the first 3 floors and the walls of the last 4 floors, and For the 22-floor structure, the changes of the moment around strong and weak flexural moment are intense in the walls of the first 4 floors and the walls of the last 4 floors and around the weak flexural axis of the walls of the first 4 floors. The maximum flexural moment on the first floor of the 12 and 22-floor structures caused by the earthquake DBE, are about 2.9 and 3.2 times greater than that amount is in the linear analysis (Bearing in mind that half of the non-linear model is considered in the non-linear analysis), respectively. According to the results of the earthquake DBE it can be said for both of the 12 and 22 floor structures that the first mode of behavior governs the structure behavior, and no effects of higher modes are seen. Fig. 16 and 17 show the mean maximum flexural moment of the shear wall no. 1 in two directions, under the earthquake of DBE and MCE for the 12 and 22-floor structures.

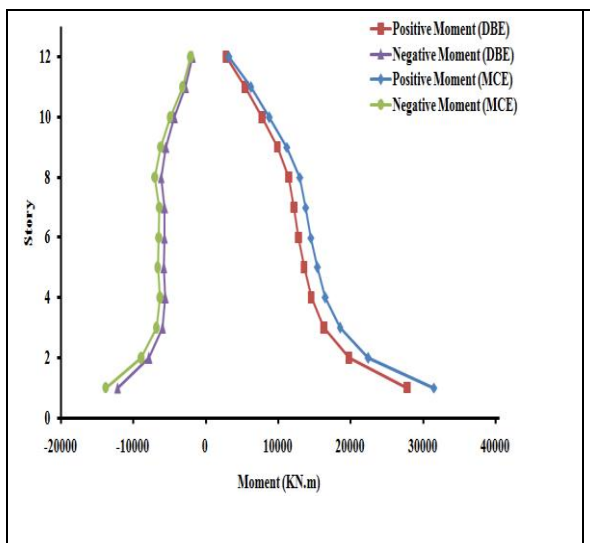


Fig. 16 mean maximum flexural moment of the shear wall no. 1 in two directions, under the earthquake of DBE and MCE for the 12 floor structure

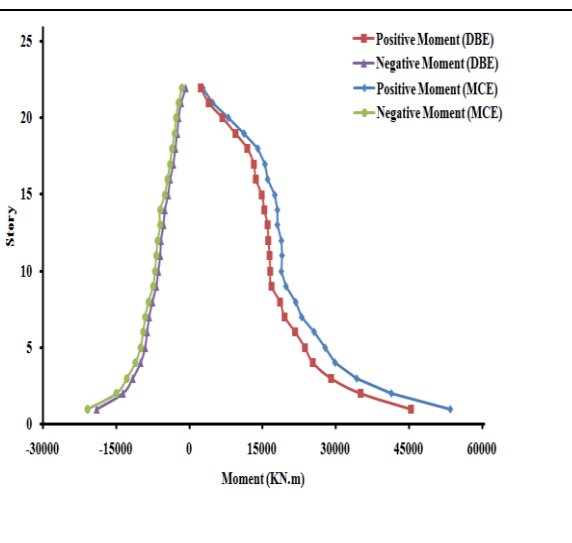


Fig. 17 mean maximum flexural moment of the shear wall no. 1 in two directions, under the earthquake of DBE and MCE for the 22 floor structure

4.3 Behavior of Steel Coupling Beams

Fig. 18 and 19 show the mean maximum rotation of the steel coupling beams for various floors in both of the 12 and 22-floor structures in earthquakes DBE and MCE.

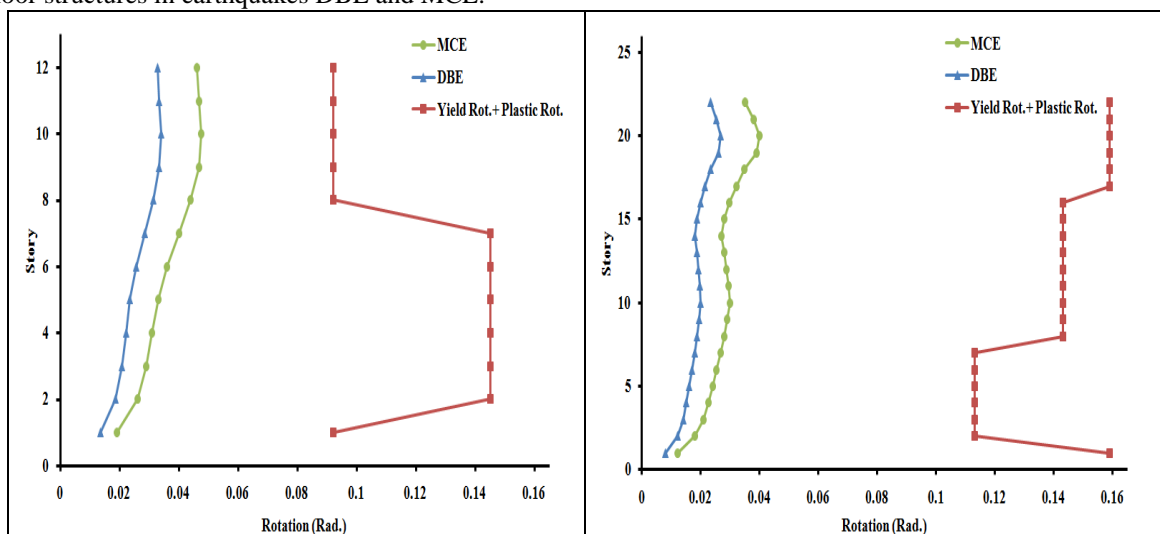


Fig. 18 mean maximum rotation of the steel coupling beams for various floors in both of the 12 floor structure in earthquakes DBE and MCE

Fig. 19 mean maximum rotation of the steel coupling beams for various floors in both of the 22 floor structure in earthquakes DBE and MCE

As you can see, all the steel coupling beams in the 12 and 22 floor structures (except for the beams of the first floor of the 22-floor structure) have submitted, but they have not experienced their maximum strength. Demand for plastic rotation on the steel coupling beams is much less than the capacity of the beams; this is due to the high stiffness and strength of shear walls that have transferred a little rotation to the coupling beams.

Fig. 20 and 21 show the mean maximum shear of the steel coupling beams in different floors of the 12 and 22-floor structures in the earthquakes DBE and MCE. As you can see, all steel coupling beams have reached yielding.

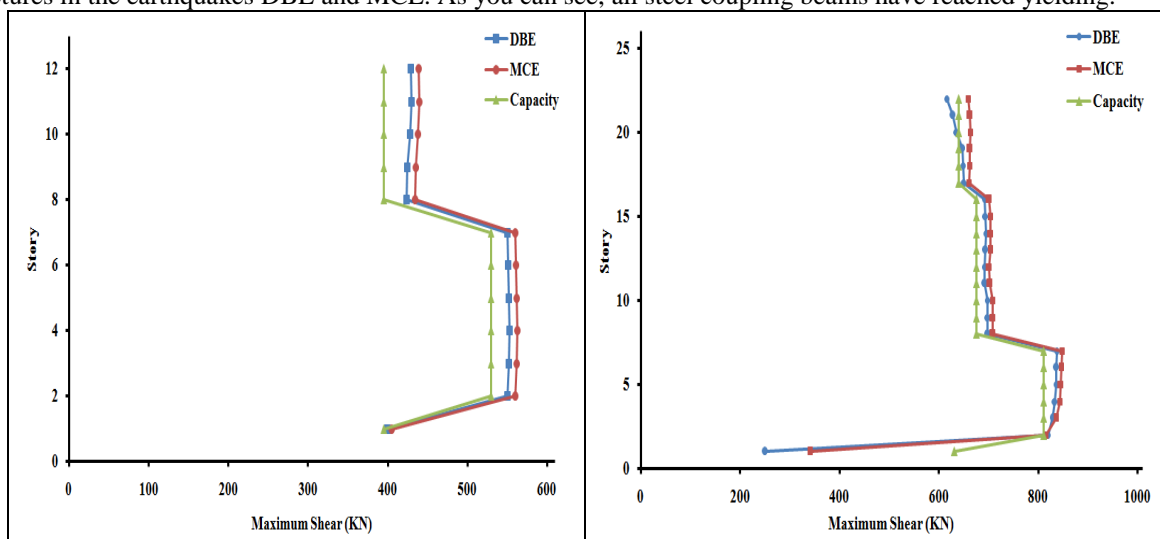


Fig. 20 mean maximum shear of the steel coupling beams in different floors of the 12 floor structure in the earthquakes DBE and MCE

Fig. 21 mean maximum shear of the steel coupling beams in different floors of the 22 floor structure in the earthquakes DBE and MCE

## 5. CONCLUSIONS

According to studies conducted on the two 12 and 22-floor structures, the following results were obtained:

- In the linear analysis and seismic DBE analysis, the percentage of the steel flexure frame and the shear walls of the total shear is about 15% and 85%. According to the nonlinear static analysis results, the percentage of the steel flexure frame of the total shear can reach more than 30% in the target displacement point.
- According to the seismic DBE results, all of the steel beams in the both 12- and 22-storey structures have reached the yield point, which is consistent with the linear analysis results (except the coupled beam of the first floor in the 22-storey structure). The rotation of the coupled beams in the 22-storey structure is more consistent with the results of the non-linear static analysis compared with the 12-floor structure.
- In both the 12 and 22-storey structures under the earthquakes DBE and MCE the rate of demand is much less than the plastic rotation capacity of the coupled beams of the floors which could be due to the high hardness and resistance of the shear walls which transfers little rotation to the coupled beams.
- Based on the results of the earthquake DBE and MCE in the 22-floor structures, the shear walls of the top floors, unlike the results of the linear analysis, bear a low tensile force.
- Based on the results of the static linear analysis and the nonlinear dynamic analysis, in both 12 and 22-floor structures, the moment direction of the shear walls has changed at the height of the structure (joint formation in the along the structure), which causes a huge waste of energy.
- According to the seismic DBE results, all of the steel beams in the both 12- and 22-storey structures have reached the yield point, which is consistent with the linear analysis results (except the coupled beam of the first floor in the 22-storey structure).

## REFERENCES

- Aktan A. E. and Bertero V. V. (1981).** The seismic resistant design of R/C coupled shear walls. *Report No. UCB/EERC-81/07, Earthquake Engineering Research Center, University of California, Berkeley.*
- Aktan A. E. and Bertero V. V. (1984).** Seismic response of R/C frame- wall structures. *ASCE Journal of the Structural Division*, 110 (ST 8), 1803- 1821.
- Aristizabal-Ochoa J. D. (1982).** Dynamic response of coupled wall systems. *ASCE Journal of The Structural Division*, 108 (ST 8): 1846-1857.
- El-Tawil S. Kuenzli C. M. and Hassan M. (2002).** Pushover of hybrid coupled walls. Part I: Design and modeling . *Journal of Structural Engineering*. 128(10): 1272-1281.
- El-Tawil S. and Kuenzli C. M. (2002).** Pushover of hybrid coupled walls. Part II: Analysis and behavior. *J. Structural Engineering*. 128(10): 1282-1289.
- El-Tawil S. Harries K. A. Fortney P. J. and Shahrooz, B. M. and Kurama, Y. (2010).** Seismic design of hybrid coupled wall systems- State of the art. *J. Structural Engineering*. 136(7), 755-769.
- FEMA-450 (2003), NEHEP Recommended Provisions for Seismic Regulations for New Buildings and Other Structures. Part I - Provisions,** Building Seismic Safety Council, Washington, D.C.
- Fintle M. and Ghosh S. K. (1982).** Case study of aseismic design of a 16- story coupled wall using inelastic
- Fortney P. J. (2005).** The next generation of coupling beams. *Disertation, University of Cincinnati, Cincinnati.*
- Harries K. A. and Mitchell D. Cook W. d. and RedWood R.G. (1993).** Seismic response of steel beams coupling reinforced concrete walls. *ASCE J. Structural Div.* 119(ST 12): 3611-3629.
- Harries, K. A., Cook, W. d., Mitchell, D., and RedWood, R.G. (1995).** The use of steel beams to couple concrete walls, *Proceedings of The Seventh Canadian Conference on Earthquake Engineering*, Montreal, Canada, 509-516.
- OpenSees (2012).** Open System for Earthquake Engineering Simulation. *Pacific Earthquake Engineering Res. Center (PEER)*. Computer Program.
- Park R. and Paulay, T. (1975).** Reinforced Concrete Structures. *John Wiley and Sons, Inc., New York.*
- Park W. S. and Yun, H. D. (2005).** Seismic behaviour of steel coupling beam linking reinforced concrete shear walls. *Engineering Structures*. 27: 1024-1039.
- Park W. S. and Yun H. D. (2005b).** Seismic behaviour of coupling beams in a hybrid coupled shear walls. *J. Constructional Steel Research*. 61:1492-1524.
- Park W. S. and Yun H. D. (2006a).** Seismic behavior and design of steel coupling beams in a hybrid coupled shear wall systems. *Nuclear Engineering and Design*. 236: 2474-2484.